

3-1-2022

PKC ϵ Activation Restores Loss of PKC ϵ , Manganese Superoxide Dismutase, Vascular Endothelial Growth Factor, and Microvessels in Aged and Alzheimer's Disease Hippocampus

Guetchyn Millien

Huaixing Wang

Zongxiu Zhang

Dan L Alkon

Jarin Hongpaisan

Follow this and additional works at: <https://jdc.jefferson.edu/transmedfp>

 Part of the [Translational Medical Research Commons](#)

[Let us know how access to this document benefits you](#)

This Article is brought to you for free and open access by the Jefferson Digital Commons. The Jefferson Digital Commons is a service of Thomas Jefferson University's [Center for Teaching and Learning \(CTL\)](#). The Commons is a showcase for Jefferson books and journals, peer-reviewed scholarly publications, unique historical collections from the University archives, and teaching tools. The Jefferson Digital Commons allows researchers and interested readers anywhere in the world to learn about and keep up to date with Jefferson scholarship. This article has been accepted for inclusion in Center for Translational Medicine Faculty Papers by an authorized administrator of the Jefferson Digital Commons. For more information, please contact: JeffersonDigitalCommons@jefferson.edu.



PKC ϵ Activation Restores Loss of PKC ϵ , Manganese Superoxide Dismutase, Vascular Endothelial Growth Factor, and Microvessels in Aged and Alzheimer's Disease Hippocampus

OPEN ACCESS

Guetchyn Millien¹, Huaixing Wang¹, Zongxiu Zhang¹, Dan L. Alkon² and Jarin Hongpaisan^{1*}

Edited by:

Zhendong Liu,
Shandong First Medical University,
China

Reviewed by:

Abhik Sen,
Rajendra Memorial Research Institute
of Medical Sciences, Indian Council
of Medical Research, India
Guoyuan Qi,
University of Arizona, United States

***Correspondence:**

Jarin Hongpaisan
jarin.hongpaisan@jefferson.edu

Specialty section:

This article was submitted to
Alzheimer's Disease and Related
Dementias,
a section of the journal
Frontiers in Aging Neuroscience

Received: 15 December 2021

Accepted: 07 February 2022

Published: 01 March 2022

Citation:

Millien G, Wang H, Zhang Z,
Alkon DL and Hongpaisan J (2022)
PKC ϵ Activation Restores Loss
of PKC ϵ , Manganese Superoxide
Dismutase, Vascular Endothelial
Growth Factor, and Microvessels
in Aged and Alzheimer's Disease
Hippocampus.
Front. Aging Neurosci. 14:836634.
doi: 10.3389/fnagi.2022.836634

¹ Center for Translational Medicine, Department of Medicine, Sidney Kimmel Medical College, Thomas Jefferson University, Philadelphia, PA, United States, ² Neurotrope Bioscience, Inc., New York, NY, United States

Vascular endothelial dysfunction and capillary loss are currently considered to be a primary phenotype of normal human aging and Alzheimer's disease (AD). Activation of protein kinase C (PKC ϵ) improves several molecular, cellular, physiological, and behavioral endpoints, yet it is not known whether a loss of PKC ϵ activity occurs in the microvascular endothelium in aged and AD hippocampi, whether this loss contributes to microvascular change, or whether activation of PKC ϵ protects against microvascular damage, an early change that induces age-associated memory defect and AD. We investigated the effect of the PKC ϵ activation on microvascular loss in the hippocampus, important for memory storage. In cultured human brain microvascular endothelial cells, tert-butyl hydroperoxide induced oxidative stress and a decrease in manganese superoxide dismutase (MnSOD) mRNA and protein expression that were blocked by the antioxidant drugs. The PKC ϵ activators bryostatin and DCPLA methyl ester increased PKC ϵ , associated with an increase in MnSOD mRNA and its protein as well as vascular endothelial growth factor (VEGF), which was inhibited by the mRNA-stabilizing HuR inhibitors. In rats (>24 months old) and AD transgenic mice Tg2576 (5 months old), bryostatin or DCP-LA prevented a decrease in vascular PKC ϵ , MnSOD, and VEGF and prevented microvascular loss and age-related memory impairment. An autopsy-confirmed AD hippocampus showed a decrease in PKC ϵ and MnSOD mRNAs and their proteins and VEGF as well as in microvascular density compared to non-AD controls. In conclusion, the PKC ϵ activation can rescue a decrease in PKC ϵ , MnSOD, and VEGF *via* posttranscription regulation and alleviate oxidative stress, and in doing so, prevent microvascular loss during aging and AD.

Keywords: aging, Alzheimer's disease, hippocampus, PKC ϵ , oxidative stress, microvessel

INTRODUCTION

Cerebral rarefaction of capillaries and terminal arterioles results in reduced microcirculation and hypoxia, often attributed to neurodegeneration and currently considered to be a primary phenotype of normal human aging and Alzheimer's disease (AD) (Kemper et al., 1999; Riddle et al., 2003; Desai et al., 2009; Arvanitakis et al., 2011; Brown and Thore, 2011; Toda, 2012; Ungvari et al., 2018). In addition, disruption of the blood-brain barrier (BBB) has been shown to prevent the clearance of amyloid beta ($A\beta$), which is known to increase during aging and AD, not only leading to amyloid plaque deposition, but also an increase in oxidative stress, inflammation, and cerebrovascular damage (Hawkes et al., 2011; Qosa et al., 2014). Moreover, oxidative damage is considered another main driving force in the aging process as well as in AD pathogenesis (Harman, 1956; Numomura et al., 2001; Sanz and Stefanatos, 2008). Therefore, drugs targeting microvascular (MV) damage and oxidative stress may be candidates for treating age-related memory impairment and AD (Kaan et al., 2013).

The three prime untranslated region (3'-UTR) is the section of messenger RNA (mRNA) that immediately follows the translation termination codon. The 3'-UTR often contains regulatory regions that post-transcriptionally influence gene expression. Protein kinase C (PKC) can activate the nuclear export and transport of the mRNA-stabilizing embryonic lethal, abnormal vision (ELAV), *Drosophila*-like, or human antigen (Hu) family proteins (HuR, HuB, HuC, and HuD) that will bind with AU-rich (ARE) sequence in the 3'-UTR, resulting in the inhibition of mRNA degradation (Chung et al., 1997; Antic and Keene, 1998; Quattrone et al., 2001; Pascale et al., 2004, 2005). The 3'-UTRs of human manganese superoxide dismutase (MnSOD) and vascular endothelial growth factor A (VEGF-A or VEGF) have multiple ARE sequences (King, 2000; Wang et al., 2001; Chaudhuri et al., 2012; Arcondeguy et al., 2013). HuR protein prevents VEGF mRNA degradation that enhances VEGF protein synthesis in vascular endothelial cells (Arcondeguy et al., 2013).

PKC ϵ and PKC α isozymes may promote the transcription of the mitochondrial antioxidant MnSOD in human lung cells and acute myeloid leukemia (Chung et al., 2011; Di Marcantonio et al., 2018). PKC ϵ can increase expression of VEGF outside of the brain (Amadio et al., 2012). Others have reported that PKC ϵ stimulates cardiovascular endothelial cell proliferation and angiogenesis (Davis et al., 2007); protects against oxidative damage, inflammation, and apoptosis (Chattopadhyay et al., 2014); and supports endothelial integrity *via* tight junctions (Sonobe et al., 2009).

A decrease in PKC activity has also been observed in the aging brain at the level of the whole hippocampus (Battaini and Pascale, 2005; Govoni et al., 2010). Down-regulation of PKC ϵ isozyme occurs at the neuronal cell or structural level in the hippocampal CA1 area in aged rats (Hongpaisan et al., 2013). Synaptic formation in the hippocampal CA1 area is important for spatial memory retention, and synaptic loss in this hippocampus is associated with age-related memory impairment (Hongpaisan and Alkon, 2007; Hongpaisan et al., 2013). Additionally, down-regulation of MnSOD, parallel to elevation of oxidative stress,

is evident during aging (El Assar et al., 2013). Loss of PKC ϵ occurs in AD neurons (Hongpaisan et al., 2013; Sen et al., 2018). Activation of PKC ϵ improves several molecular, cellular, physiological, and behavioral endpoints, including degradation of $A\beta$, prevention of synaptic loss, induction of synaptogenesis, and prevention of cognitive deficits and memory loss (Hongpaisan et al., 2011; Sen et al., 2012).

It is not known whether a loss of PKC ϵ activity also occurs in the MV endothelium in aged and AD hippocampi, whether this loss contributes to MV change, or whether activation of PKC ϵ protects against MV damage, which is one of several early changes that induce age-associated memory defect and AD. In the present study, we studied the effects of the PKC ϵ activator and peroxide tert-butyl hydroperoxide (TBHP)-induced oxidative stress on PKC ϵ , MnSOD, and VEGF in human brain MV endothelial cells (HBMEC) in cultures. We also measured changes in PKC ϵ , MnSOD, and VEGF in microvessels associated with MV density in the hippocampus and the therapeutic effects of the PKC ϵ activators 8-(2-(2-pentyl-cyclopropylmethyl)-cyclopropyl)-octanoic acid (DCP-LA) and bryostatin in age-related memory impaired rats, AD transgenic mice Tg2576, and/or autopsy-confirmed AD human subjects. Change in microvessels was focused in the stratum radiatum of the dorsal hippocampal CA1 area, comprising apical dendrites of the CA1 pyramidal neurons. Changes in dendritic spine morphology and synaptic density in the dorsal hippocampus – particularly the generation of mushroom spines and synapses within the apical dendrites of CA1 pyramidal neurons – are correlated with changes in spatial memory (Hongpaisan and Alkon, 2007).

MATERIALS AND METHODS

Cell Culturing

Human brain MV endothelial cells (Neuromics, Edina, MN, United States, cat # HEC02 or ScienCell Research Laboratories, Carlsbad, CA, United States, cat # 1000) at subculture passage 2–5 were grown on fibronectin-coated cover glasses (0.8 mm diameter) in 12-well plates or fibronectin-coated 6-well plates. Cultured cells were maintained in endothelial medium (ScienCell) supplemented with the endothelial cell growth supplement (ECGS, ScienCell) and 5% fetal calf serum up to 3 days at about 1 ml per well (3.5 cm² surface area) on the 12-well plate or 3 ml per well (9.6 cm² surface area) on the 6-well plate. Because unlike most other cell types, HBMEC could not survive under serum-free medium to induce maturity, the limited culture medium and fetal calf serum, without fresh culture medium change, allowed HBMEC cells to initially multiply and thereafter reach maturity during the gradual exhaustion of serum. For immunohistochemistry, cultured cells growing on cover glasses were fixed with 4% paraformaldehyde at room temperature for 15–20 min and kept in phosphate buffered saline (PBS) at 4°C.

Measurement of Superoxide

The specific probe hydroethidine (Thermo Fisher Scientific, Waltham, MA, United States, cat # D11347) was used to measure changes in cellular superoxide ($O_2^{\bullet-}$) production

(Sen and Hongpaisan, 2018). The reaction between O₂^{•-} and non-fluorescent hydroethidine generates a highly specific red fluorescent product, 2-hydroxyethidium. In biological systems, another red fluorescent product ethidium is also formed, usually at a much higher concentration than 2-hydroxyethidium (Zielonka and Kalyanaraman, 2010). Cultured cells, grown on glass slides, were incubated with hydroethidine (2 μ g/ml) at room temperature for 15–20 min and then fixed with 4% paraformaldehyde. Increased O₂^{•-} production was qualitatively determined with a confocal microscope at 488 nm/>510 nm (excitation/emission).

Aged Rats With Learning Impairment

Brown Norway rats were obtained from the National Institute on Aging, National Institutes of Health (NIH) facilities (Harlan, Indianapolis, IN, United States). Animals were housed in an animal facility for 1 month prior to experiment to recover from transport. Young rats (5 months) and aged rats (>24 months) were trained in a water maze pool, as previously described (Hongpaisan et al., 2013). In short, rats were trained to find a platform hidden by dissolving non-toxic white tempera (BesTemp; Certified Color Corp., Orange, CA, United States) in the water (two swims per day for 5 days). Aged rats were divided into two groups: (1) aged, learning-unimpaired group; and (2) aged, learning-impaired group (Hongpaisan et al., 2013). Only aged, learning-impaired rats were used in the present study. Rats were injected with the PKC ϵ activators (5 μ g/kg bryostatin [MilliporeSigma, Burlington, MA, United States, cat # 203811] or 1.5 mg/kg DCP-LA [MedChemExpress, Monmouth Junction, NJ, United States, cat # HY-108599A] diluted with normal saline, i.p., every other day for five injections before and three more injections during spatial memory training), compared to young and aged rats injected with normal saline (in the absence of the PKC ϵ activator). Ten days after the first 5-day swim, rats were trained for the second 5-day swim. At 24 h later, the probe test was carried out to test the memory of rats to concentrate their swimming on the removed platform area.

Alzheimer's Disease Transgenic Mice

Male Tg2576 [Genotype: Hemizygous for 129S6.Cg-Tg(APP^{SWE})2576Kha N20] and wild-type control mice (approximately 2 months old) were purchased from Taconic (Hudson, NY, United States) and housed for 1 week before the experiment to recover from transport stress. Bryostatin, kindly provided by the National Cancer Institute (NCI), NIH (Bethesda, MD, United States), was administered in 2 doses/week for 14 weeks (30 μ g/kg body weight, dissolved in sterile normal saline, i.p.). Non-treated groups received the same volume of normal saline, mechanism of delivery, and frequency of administration as the treated groups.

Animal Brain Tissue Preparation

Rats and mice were deeply anesthetized with sodium pentobarbital (120 mg/kg body weight, i.p.). Animals were perfused through the heart with cold PBS for less than 4 min to wash out the blood and subsequently with 4% paraformaldehyde in PBS. Brains were then removed, postfixed for 20 min, and

stored in PBS at 4°C. Under the stereoscope, the right brain was dissected, and the midbrain and cortex part were removed to expose the hippocampus. The right dorsal hippocampus and cerebral cortex were excised. A small piece of filter paper partially wet with PBS was used to remove excessive PBS and to transfer tissue to mount on the vibratome stage with super glue that was spread to a thin layer with another dried filter paper. Using the remaining cerebral cortex as the support, the hippocampus was sectioned with a vibratome (Leica VT1200S; Leica Microsystems, Wetzlar, Germany) into 200 μ m (for mouse) or 300 μ m (for rat) thickness and kept in series in PBC at 4°C. The hippocampal cross-sections were excised from the serial sections; #1, #4, #7, and #9 (400 μ m apart for mouse or 600 μ m apart for rat) were further fixed in 4% formaldehyde in PBS at 4°C overnight to harden the tissue. The 200 or 300- μ m thickness tissue section was mounted on a vibratome stage with a thin layer of super glue and then cut again with the vibratome into 5 μ m thickness by adjusting the suitable knife angle, sectioning arm speed, and vibrating frequency. Four hippocampal sections at 5- μ m thickness were then processed free-floating for immunohistochemistry and cytochemistry. A watercolor painting brush #0 trimmed to have just a couple of hairs was used to carry thin tissue sections from the buffer bath of vibratome. Tissue sections (clear of excessive glue) were immersed with the painting brush to attach the container floor without rocking or shaking during antibody incubation or washing to prevent the sections floating on the surface of solution.

Human Brain Tissue Preparation

The pathological diagnosis of AD was conducted according to the Consortium to Establish a Registry for Alzheimer's Disease (CERAD). All patients (or relatives/representatives who had the power of attorney) signed informed consent forms. The present work was carried out in accordance with the Code of Ethics of the World Medical Association (Declaration of Helsinki) for experiments involving humans¹. Autopsied brains were fixed in 10% formalin. Human hippocampal samples at 0.4 cm thickness were processed for paraffin embedding. Paraffin-embedded sections (10 μ m) were mounted on glass slides and deparaffinized with xylene (two times; 5 min each) and 100% ethanol for 5 min. Tissue sections were then rehydrated with graded alcohol. For antigen retrieval of human autopsies, deparaffinized hippocampal sections were incubated in 10 mM citrate buffer pH 6.0 added with 0.05% Tween at 95°C for 30 min.

Immunohistochemistry, Cytochemistry, and Confocal Microscopy

Tissue specimens were treated with Image-iTTM FX signal enhancer (Thermo Fisher Scientific, Waltham, MA, United States) for 30 min and PBS containing 15% serum and 0.5% Triton X-100 for 60 min at room temperature, to block non-specific protein binding sites. For primary antibody incubation, specimens were incubated overnight at room temperature,

¹<http://www.wma.net/en/30publications/10policies/b3/index.html>

except that human tissue were incubated at 4°C for 3 days and at room temperature for 24 h. Primary antibodies are anti-PKC ϵ (rabbit polyclonal IgG; 1:100; MilliporeSigma, Burlington, MA, United States, Cat # 06-991), platelet/endothelial cell adhesion molecules-1 (PECAM or CD31, goat polyclonal antibody, Santa Cruz Biotechnology, Dallas, Tx, United States, cat # sc-37664), anti-PKC α (mouse monoclonal IgG; 1:100; MilliporeSigma, Burlington, MA, United States/Upstate, cat # 23336), anti-MnSOD (rabbit polyclonal IgG; 1:100; MilliporeSigma, Burlington, MA, United States, cat # 06-984), and anti-VEGF (mouse monoclonal IgG; 1:50; Santa Cruz Biotechnology, Dallas, Tx, United States, cat # sc-7269). Specimens were then incubated with biotinylated horse anti-mouse antibody (1:20; Vector Laboratories, Burlingame, CA, United States, cat # BA-2000) and/or Alexa Fluor 568 donkey anti-rabbit (cat # A10042) or goat (cat # A11057) antibody (1:200; Thermo Fisher Scientific, Waltham, MA, United States) for 3 h at room temperature. For blood vessel staining, rodent tissue sections were incubated with biotin-conjugated isolectin B4 (IB4) from *Bandeiraea simplicifolia* (*Griffonia simplicifolia*, 1:50; Vector Laboratories, Burlingame, CA, United States, cat # B-1205) at room temperature for 4 h. Tissue sections treated with biotinylated antibody or lectin were incubated with Alexa Fluor 488 streptavidin (1:100; Thermo Fisher Scientific, Waltham, MA, United States, cat # S11223A) for 3 h at room temperature. After each lectin and/or antibody incubation, the samples were washed with PBS three times (each time for a period of 5 min). Sections were mounted with VECTASHIELD mounting medium with DAPI (Vector Laboratories, Burlingame, CA, United States) to counterstain nuclei. For negative controls, primary or secondary antibodies were replaced with protein with no antigenicity against the tested antibody.

Hippocampal slices were oriented with a Zeiss Axio Observer Z1 microscope equipped with a 710 confocal scanning system using the 10x objective lens in the DAPI channel (for staining nuclei). The random CA1 area that appeared immediately after switching to the higher magnification lens, either 63X or 100x Plan-APO Chromat oil immersion objectives (1.4 NA), was imaged for appropriate fluorescence (e.g., Alexa 488 and/or 568). Confocal images of hippocampal sections were acquired in line scan mode with a pinhole of approximately 1.00 Airy unit and averaged data from several images were reported.

Quantitative Analysis of Immunohistochemistry

Protein expression was determined with semi-quantitative analysis. All tissue samples within the same experiment were processed for immunohistochemistry at the same time and imaged with the same set-up of confocal microscope (the same objective lens, digital magnification, etc.) within the same day. At least five images were randomly collected from each culture, animal, and human brain. The confocal images were transferred to quantify them in another computer with the ImageJ program². The individual image was collected at 1024 pixels \times 1024 pixels. For individual analysis, a group of eight bits was assigned

²<http://rsb.info.nih.gov/ij/>

one of the 225 possible integers from 0 to 255 to each pixel. Individual cells were identified with specific immune-expression (Alexa 488 or 568) to stain the target proteins and their DAPI-stained nucleus. The border of each individual cultured cell was rather clear, while the border between two adjacent cells in the *in situ* microvessels was imagined at the middle line between 2 different nuclei. Under ImageJ program, regions of interest (ROI) of each individual cell were manually drawn and analyzed for the mean gray intensity value from the pixels of:

1. Alexa 488 or 568 within the cell area (the cytosol and nucleus together) for target protein, except for mitochondrial MnSOD (only in the cytoplasm), and
2. DAPI within the nuclear area.

Data were collected at a single cell level (Alexa 488 or 568 intensity of the target protein normalized with its nuclear DAPI intensity). Data were averaged from the overall cells collected under the same experiment group. The averaged control data were set at 100%, and all other experiment data were defined as % of their controls.

Cell Lysis and Western Blot Analysis

Cultured cells were harvested in homogenizing buffer (HB) containing 10 mM Tris-Cl (pH 7.4), 1 mM PMSF (phenylmethylsulfonylfluoride), 1 mM EGTA, 1 mM EDTA, 50 mM NaF, 20 μ M leupeptin, and 1% Triton X-100 and were lysed by sonication. Protein concentration was measured using the Coomassie Plus (Bradford) Protein Assay kit (Pierce, Rockford, IL, United States). About 20 μ g of protein from each sample was subjected to SDS-PAGE analysis in a 4–20% gradient Tris-glycine polyacrylamide gel (Invitrogen, Waltham, MA, United States). The separated protein was then transferred to a nitrocellulose membrane, blocked with BSA, and incubated at 4°C overnight with primary antibodies: anti-PKC ϵ (rabbit polyclonal IgG; 1:500; Novus Biologicals, Littleton, CO, United States, NBP2-19848), anti-MnSOD (mouse monoclonal IgG; 1:1,000; MilliporeSigma, Burlington, MA, United States, cat # 06-984), anti-VEGF (rabbit polyclonal IgG; 1:500; Invitrogen, Waltham, MA, United States, cat # PA1-16948), anti- β -Actin (mouse monoclonal IgG; 1:25,000, Millipore, MABT825 or rabbit polyclonal IgG; 1:25,000, Novus Biologicals, Littleton, CO, United States, NBP2-7636). After being washed three times with TBS-T (Tris-buffered saline-Tween 20), the membrane was further incubated with alkaline phosphatase conjugated secondary antibody (1:10,000) for 45 min. The membrane was again washed three times with TBS-T and developed with the 1-step NBT-BCIP substrate (Pierce, Rockford, IL, United States). The blot was imaged in an ImageQuant RT-ECL (GE Life Sciences, Piscataway, NJ, United States), and densitometric quantification was performed using Image J software. For quantifying expression of a protein, the densitometric value for the protein of interest was normalized against β -Actin (loading control).

RNA Isolation and Quantitative PCR

Human brain MV endothelial cells cultured cells from 6-well or p100 plates were washed with 1X PBS followed by trypsinization using diluted trypsin added to each well at room temperature. Cells were observed under a microscope for complete dissociation and transferred to 1.5-ml Eppendorf tubes containing fetal bovine serum and mixed to inactivate trypsin spin at 1000 rpm for 5 min. The supernatants were removed, pellets were washed with 1 ml 1X PBS, 350 μ l RLT buffer was added, and the cells were stored at -80 for subsequent RNA isolation. Total RNA was isolated using RNeasy kit with on column DNase treatment following the manufacturer's protocol. The 1 μ g of total RNA was reverse transcribed (RT) using Omniscript (Qiagen, Germantown, MD, United States), and quantitative real-time PCR (qPCR) was performed with FAST SYBR Green or Fast TaqMan master mix (Life Technologies, Carlsbad, CA, United States) on the Step One plus ABI 7000 machine (Applied Biosystems, Waltham, MA, United States). Data were normalized to 18S. PCR assays are:

Assay name	Assay ID	Vendor
PKC epsilon (PRKCE)	HP208540	Origene
MnSOD	Hs00167309_m1	Thermofisher
B-Actin	Hs99999903_m1	Thermofisher
18S	Hs99999901_s1	Thermofisher
VEGFA	Hs00900055_m1	Thermofisher

Statistical Analysis

Data with two experimental groups, western blot, and qPCR were analyzed with Student's *t*-test. For experiments with three or more groups, data with a significant overall difference among the groups as demonstrated by ANOVA were further analyzed by Tukey multiple comparisons. The confidence level was set at 95% ($\alpha = 0.05$).

RESULTS

Effects of the PKC ϵ Activator on the Tert-Butyl Hydroperoxide-Induced Increase in Superoxide ($O_2^{\bullet-}$) Production

Oxidative damage is the main driving force in the aging process (Harman, 1956; Sanz and Stefanatos, 2008). Stable organic peroxide TBHP was used to induce mitochondrial dysfunction, leading to an increase in $O_2^{\bullet-}$ and oxidative stress (Elmlinger et al., 2011; Fedotcheva and Mokhova, 2013). Cultured HBMEC cells at 95% confluence were treated with 50, 200, or 500 μ M TBHP for 1 h and switched to the fresh culture medium without TBHP for 3 days, compared to control cells treated accordingly without TBHP. Fluorescence imaging of ethidium was used to determine $O_2^{\bullet-}$ level (Figure 1A). Intracellular $O_2^{\bullet-}$ level was increased on day 3, but not day 1, in a TBHP concentration-dependent fashion (Figure 1B). TBHP only at 500 μ M was then used in later experiment.

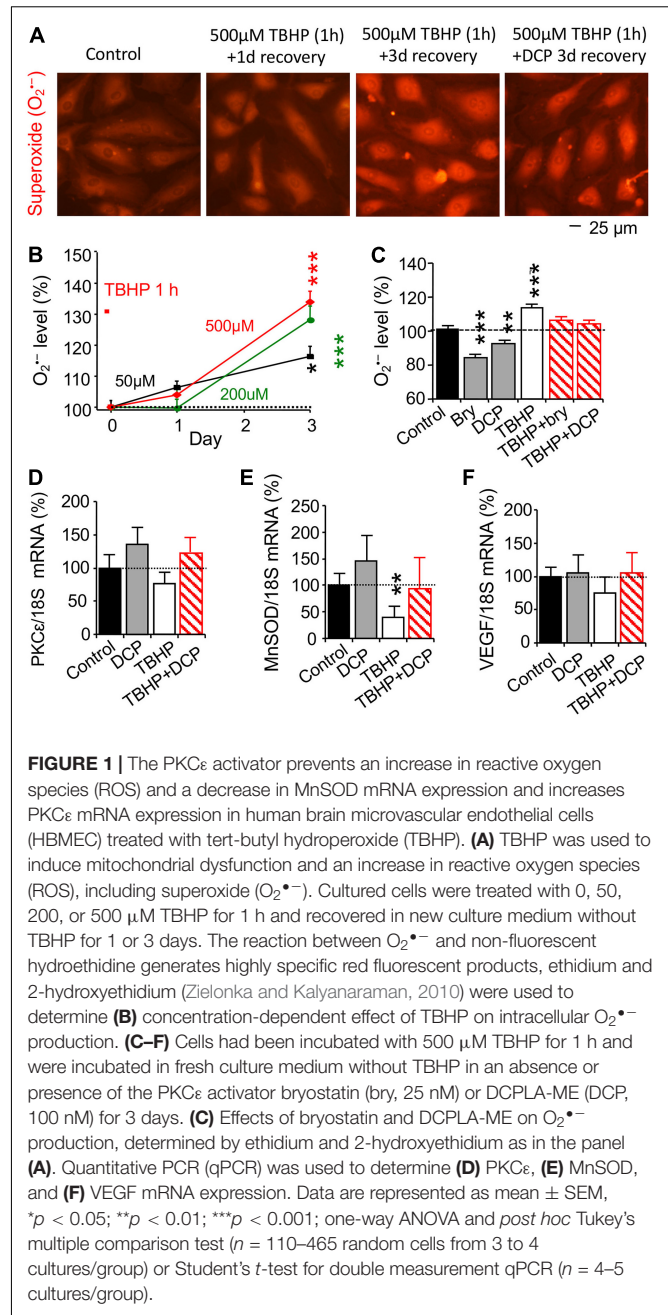


FIGURE 1 | The PKC ϵ activator prevents an increase in reactive oxygen species (ROS) and a decrease in MnSOD mRNA expression and increases PKC ϵ mRNA expression in human brain microvascular endothelial cells (HBMEC) treated with tert-butyl hydroperoxide (TBHP). **(A)** TBHP was used to induce mitochondrial dysfunction and an increase in reactive oxygen species (ROS), including superoxide ($O_2^{\bullet-}$). Cultured cells were treated with 0, 50, 200, or 500 μ M TBHP for 1 h and recovered in new culture medium without TBHP for 1 or 3 days. The reaction between $O_2^{\bullet-}$ and non-fluorescent hydroethidine generates highly specific red fluorescent products, ethidium and 2-hydroxyethidium (Zielonka and Kalyanaraman, 2010) were used to determine **(B)** concentration-dependent effect of TBHP on intracellular $O_2^{\bullet-}$ production. **(C–F)** Cells had been incubated with 500 μ M TBHP for 1 h and were incubated in fresh culture medium without TBHP in an absence or presence of the PKC ϵ activator bryostatin (bry, 25 nM) or DCPLA-ME (DCP, 100 nM) for 3 days. **(C)** Effects of bryostatin and DCPLA-ME on $O_2^{\bullet-}$ production, determined by ethidium and 2-hydroxyethidium as in the panel **(A)**. Quantitative PCR (qPCR) was used to determine **(D)** PKC ϵ , **(E)** MnSOD, and **(F)** VEGF mRNA expression. Data are represented as mean \pm SEM, * $p < 0.05$; ** $p < 0.01$; *** $p < 0.001$; one-way ANOVA and *post hoc* Tukey's multiple comparison test ($n = 110$ – 465 random cells from 3 to 4 cultures/group) or Student's *t*-test for double measurement qPCR ($n = 4$ – 5 cultures/group).

After 500 μ M TBHP for 1 h, cultured HBMEC cells were treated with the PKC ϵ activator bryostatin (25 nM, MilliporeSigma, Burlington, MA, United States) or DCPLA-ME (100 nM, MedChemExpress, Monmouth Junction, NJ, United States) for 3 days, compared with control cells treated accordingly without TBHP and the PKC ϵ activator. As summarized in **Figure 1C**, bryostatin and DCPLA-ME decreased intracellular $O_2^{\bullet-}$ level compared to the basal $O_2^{\bullet-}$ level in cells without TBHP treatment but prevented an increase in $O_2^{\bullet-}$ level in cells treated with TBHP. The results indicate that PKC ϵ activation can reduce oxidative stress.

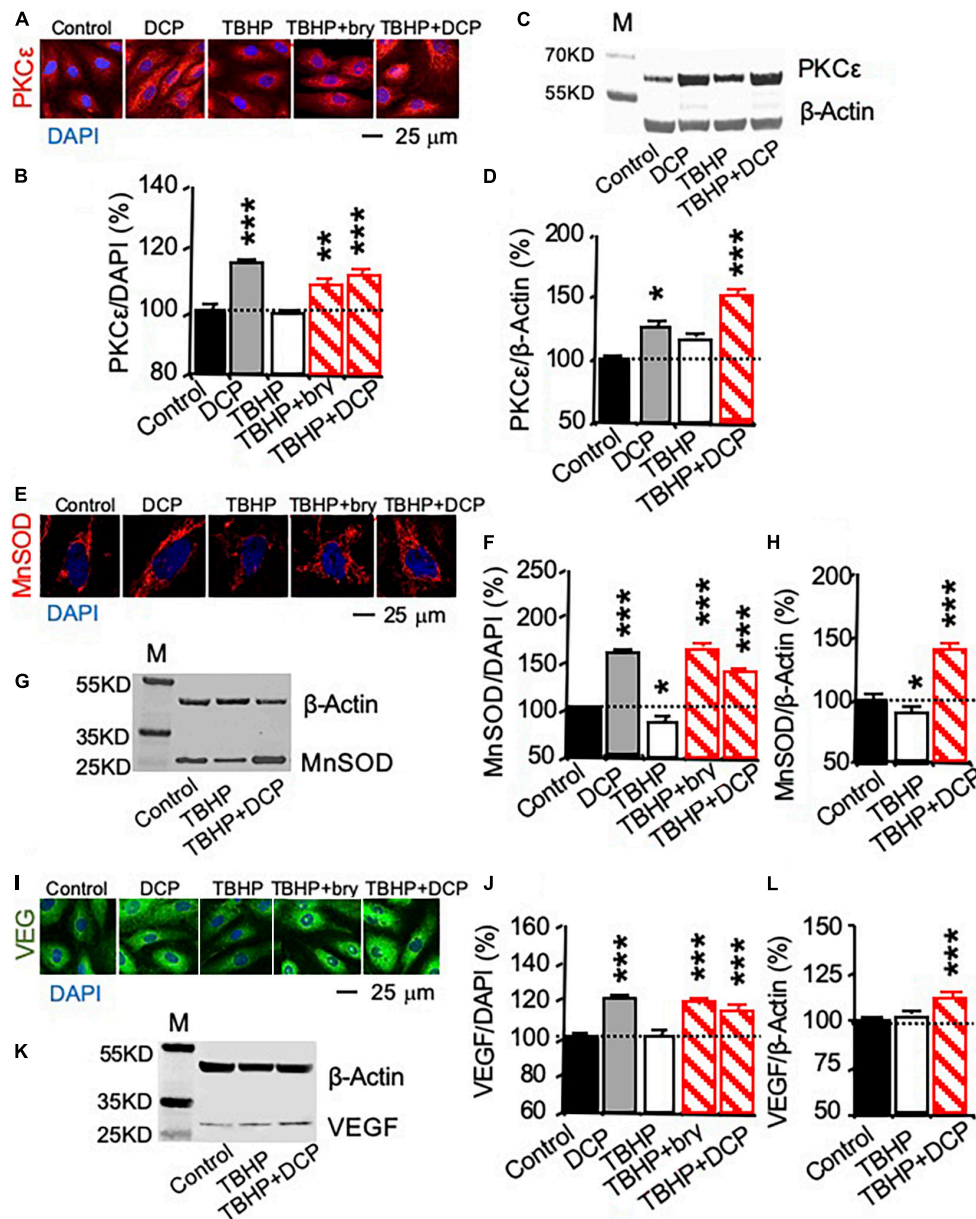


FIGURE 2 | PKC ϵ activation increases PKC ϵ , MnSOD, and VEGF protein expression in cultured human brain microvascular endothelial cells (HBMEC) treated with tert-butyl hydroperoxide (TBHP). Cultured cells were treated with 500 μ M TBHP for 1 h and incubated in new culture medium with or without the PKC ϵ activators bryostatin (bry, 25 nM) and DCPLA-ME (DCP, 100 nM) for 3 days. **(A,B,E,F,I,J)** Immunohistochemistry imaged with confocal microscopy and **(C,D,G,H,K,L)** western blot analysis of **(A–D)** PKC ϵ , **(E–H)** MnSOD, and **(I–L)** VEGF. M, molecular weight marker. Data are represented as mean \pm SEM, * p < 0.05; ** p < 0.01; *** p < 0.001; one-way ANOVA and *post hoc* Tukey's multiple comparison test (n = 59–134 MnSOD-immunostained cells or 451–907 PKC ϵ or VEGF-immunostained cells from 3 to 4 cultures/group or t-test (n = 3 cultures/western blot group).

Effect of the PKC ϵ Activator on the Tert-Butyl Hydroperoxide-Induced Change in PKC ϵ , Manganese Superoxide Dismutase, and Vascular Endothelial Growth Factor

Change in mRNA expression was studied with quantitative PCR (qPCR, **Figures 1D–F**), while protein expression was studied

with immunohistochemistry (**Figures 2A,E,I**) and western blotting (**Figures 2C,G,K**). TBHP decreased MnSOD mRNA (**Figure 1E**) and protein (**Figures 2E–H**) but had no effect on PKC ϵ (**Figures 1D, 2A–D**) and VEGF (**Figures 1F, 2I–L**) mRNA and protein expression. The results indicate that TBHP-dependent oxidative stress is correlated with a decrease in MnSOD, but not PKC ϵ and VEGF, mRNA expression and translation.

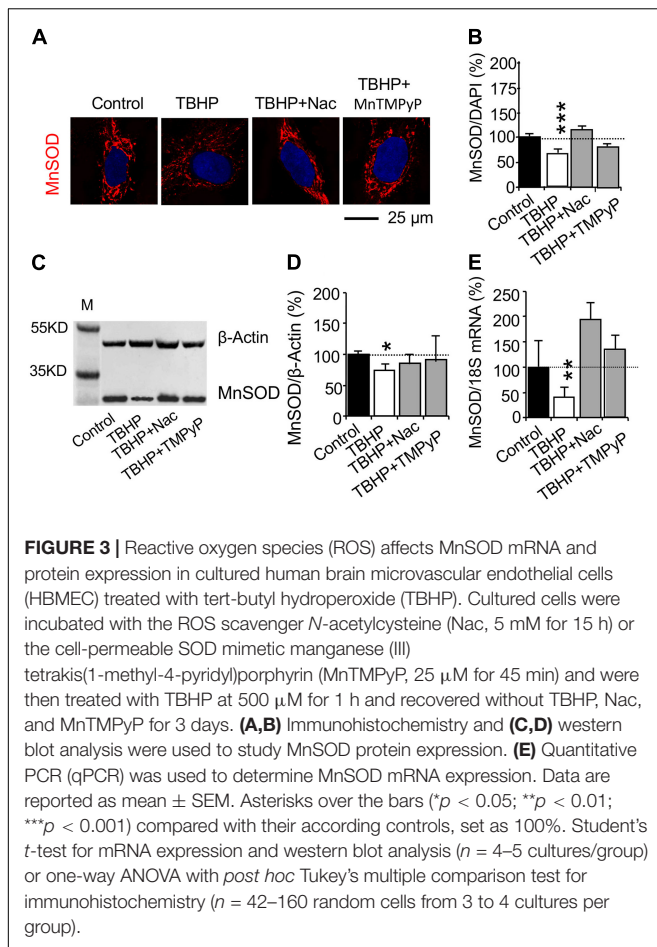


FIGURE 3 | Reactive oxygen species (ROS) affects MnSOD mRNA and protein expression in cultured human brain microvascular endothelial cells (HBMEC) treated with tert-butyl hydroperoxide (TBHP). Cultured cells were incubated with the ROS scavenger *N*-acetylcysteine (Nac, 5 mM for 15 h) or the cell-permeable SOD mimetic manganese (III) tetrakis(1-methyl-4-pyridyl)porphyrin (MnTMPyP, 25 μ M for 45 min) and were then treated with TBHP at 500 μ M for 1 h and recovered without TBHP, Nac, and MnTMPyP for 3 days. **(A,B)** Immunohistochemistry and **(C,D)** western blot analysis were used to study MnSOD protein expression. **(E)** Quantitative PCR (qPCR) was used to determine MnSOD mRNA expression. Data are reported as mean \pm SEM. Asterisks over the bars (* p < 0.05; ** p < 0.01; *** p < 0.001) compared with their according controls, set as 100%. Student's *t*-test for mRNA expression and western blot analysis (n = 4–5 cultures/group) or one-way ANOVA with *post hoc* Tukey's multiple comparison test for immunohistochemistry (n = 42–160 random cells from 3 to 4 cultures per group).

In cells without TBHP treatment, the PKC ϵ activator DCPLA-ME did not affect PKC ϵ , MnSOD, and VEGF mRNA expression (Figures 1D–F) but increased their protein translation (Figures 2B,D,E,F,J). In cells treated with TBHP, DCPLA-ME prevented the TBHP-induced decrease in MnSOD mRNA expression (Figure 1E). When compared with controls, bryostatin or DCPLA-ME in cells treated with TBHP did not increase PKC ϵ , MnSOD, and VEGF mRNAs (Figures 1D–F) but increased their protein expression (Figures 2B,D,E,H,J,L). The results suggest that PKC ϵ activation may promote PKC ϵ , MnSOD, and VEGF protein expression without the increase in their mRNA expression.

Effect of the Reactive Oxygen Species Scavengers on the Tert-Butyl Hydroperoxide-Induced Decrease in Manganese Superoxide Dismutase mRNA and Protein Expression

To verify whether the oxidative damage affect MnSOD mRNA and protein expression, cultured cells were incubated with the reactive oxygen species (ROS) scavenger *N*-acetylcysteine (Nac) or the cell-permeable SOD mimetic manganese (III) tetrakis(1-methyl-4-pyridyl)porphyrin (MnTMPyP) (Sen et al., 2018). Effect

of the superoxide scavenger Nac and the superoxide dismutase mimetic drug MnTMPyP was studied in cultured cells treated with 500 μ M TBHP for 1 h and maintained in culture medium for 3 days. Nac and MnTMPyP inhibited the effect of TBHP on the decrease in MnSOD protein expression, as determined with immunohistochemistry (Figures 3A,B) and western blot analysis (Figures 3C,D). Nac and MnTMPyP also blocked the TBHP-dependent decrease in MnSOD mRNA expression (Figure 3E). The results suggested that treatment with 500 μ M TBHP for 1 h increases ROS production and oxidative stress that decreases MnSOD mRNA expression.

Effect of the PKC ϵ -Dependent mRNA-Stabilizing Protein HuR on Manganese Superoxide Dismutase and Vascular Endothelial Growth Factor Expression

The HuR inhibitors dihydrotanshinone-I (DHTS) and CMLD-2 were used to study whether PKC ϵ activated the mRNA stabilizing protein HuR, leading to the promotion of MnSOD and VEGF expression (Lal et al., 2017; Allegri et al., 2019). To investigate whether PKC ϵ can activate HuR that can bind and chaperone the mRNA from the nucleus to the cytoplasm, immunohistochemistry was used to study the export of HuR from the nucleus to the cytoplasm during the PKC ϵ activation (Figure 4A). Bryostatin and DCPLA-ME decreased the nuclear HuR per cytoplasmic HuR ratio compared to the control level, indicating that PKC ϵ activation is associated with the nuclear export of HuR. The nuclear export of HuR was inhibited with the interfere of the specific binding of HuR to the ARE-binding sites in the mRNAs by the DHTS and CMLD-2 (Figure 4A).

Protein expression was studied with immunohistochemistry (Figures 4B,F) and western blotting, while change in mRNA expression was studied with qPCR (Figures 4C,D,G,H). The HuR inhibitors, DHTS and CMLD-2, significantly suppressed the PKC ϵ -activated increase in MnSOD protein (Figures 4B–D) as well as mRNA expression (Figure 4E). DHTS and CMLD-2 also inhibited the PKC ϵ -activated increase in VEGF expression (Figures 4F–H). The results indicate that posttranscription effect of PKC ϵ on the increase in MnSOD and VEGF expression.

Effect of the PKC ϵ Activator in Rat Hippocampus With Age-Related Memory Impairment

Rats were trained with water maze swim learning for 5 days. For learning acquisition, aged (24 months old) rats with learning impairment exhibited increased swimming (latency) time to reach the hidden platform compared to young (5 months old) adult rats (Figure 5A). Age-related learning impairment was improved by bryostatin or DCPLA-ME treatment starting on day 3 of swim learning (Figure 5A). At 24 h after the final training swim, all animals underwent a probe test to evaluate whether they remembered the location of the platform despite being removed from the test area (Figure 5B). Age-related memory-impaired rats had poor memory to swim across to the removed platform

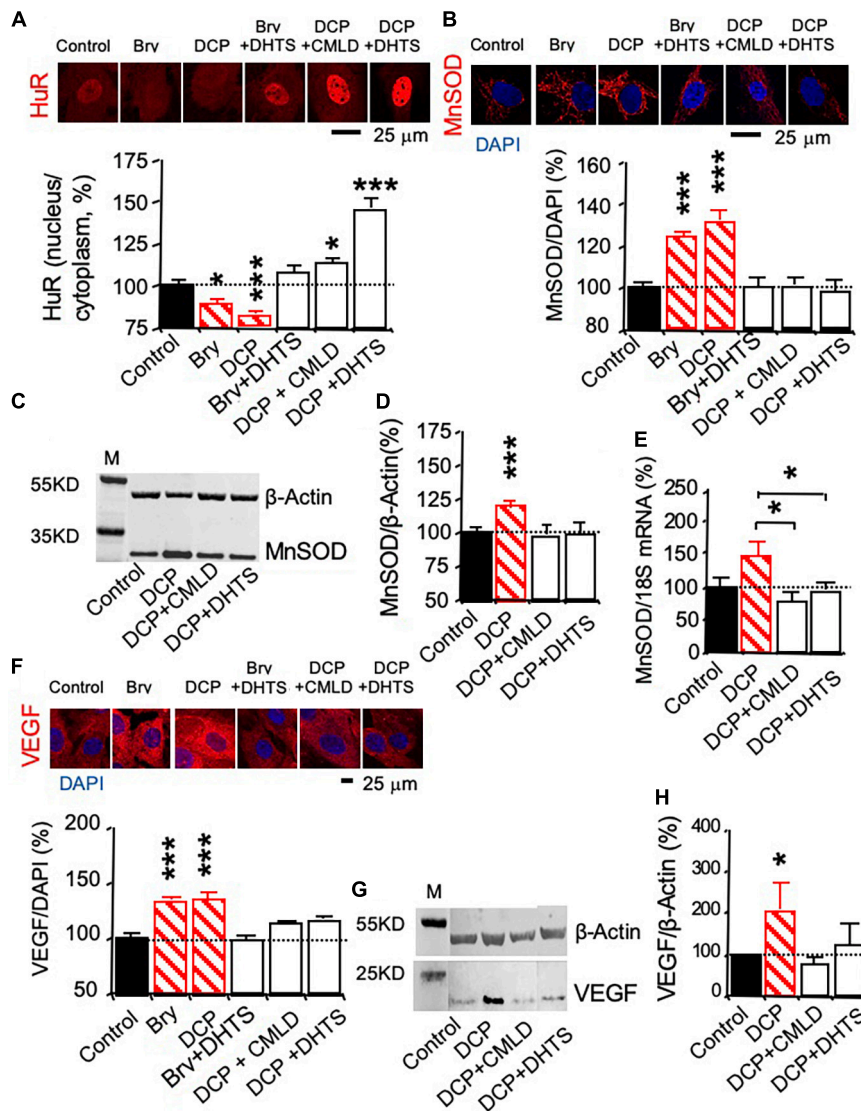
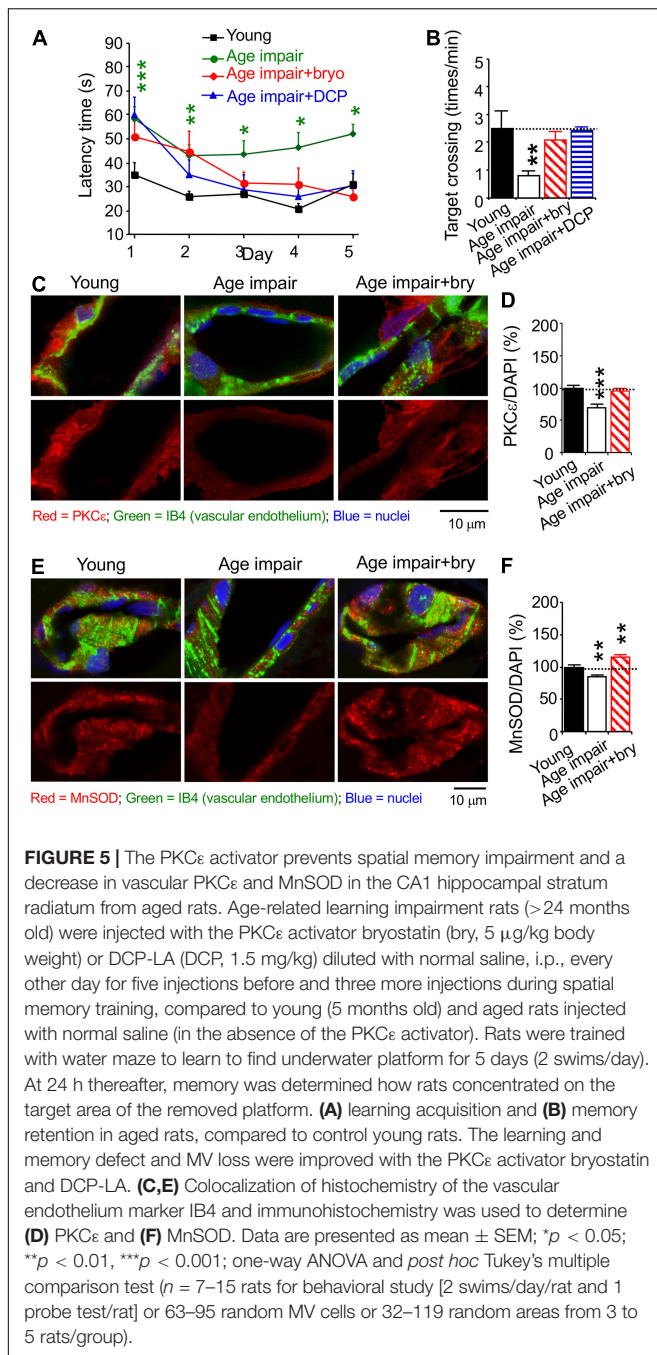


FIGURE 4 | The mRNA-stabilizing protein HuR involved in PKC ϵ -activated MnSOD and VEGF expression in human brain microvascular endothelial cells (HBMEC). HBMEC cells were treated with the HuR inhibitor CMLD-2 (35 μ M) or dihydrotanshinone-I (DHTS, 10 μ M) for 30 min before and during the 3-day incubation in the presence of the PKC ϵ activator bryostatin (25 nM) or DCPLA-ME (100 nM). **(A)** Immunohistochemistry of HuR was used to study nuclear export of the HuR protein. **(B)** Immunohistochemistry and **(C,D)** western blot analysis of MnSOD protein expression. **(E)** Quantitative PCR (qPCR) of MnSOD mRNA expression. **(F)** Immunohistochemistry and **(G,H)** western blot analysis of VEGF protein expression. M, molecular weight marker. Data are represented as mean \pm SEM, * p < 0.05; *** p < 0.001; one-way ANOVA and *post hoc* Tukey's multiple comparison test (n = 59–134 MnSOD-immunostained cells or 451–907 PKC ϵ or VEGF-immunostained cells from 3 to 4 cultures/group or *t*-test (n = 3 cultures/western blot group).

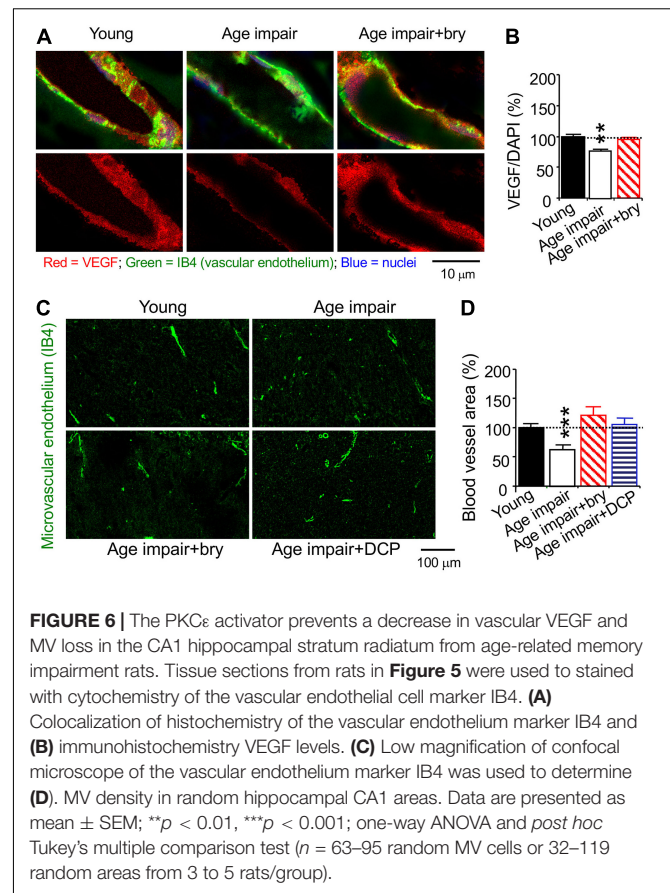
site in the water maze compared to young rats (**Figure 5B**). Bryostatin and DCP-LA increased spatial memory to the young control level (**Figure 5B**).

We studied MV density in the hippocampal CA1 stratum radiatum using the isolectin B4 (IB4), which specifically binds terminal α -galactosyl residues of vascular endothelial cells to stain MV endothelium (Laitinen, 1987; Benton et al., 2008). Confocal microscopy was used to quantify immunostained levels of PKC ϵ , MnSOD, and VEGF; each of them was colocalized with the vascular endothelial isolectin B4 (IB4), which specifically binds terminal α -galactosyl residues of vascular

endothelial cells (Laitinen, 1987; Benton et al., 2008), bound with biotin/avidin/green fluorescence dye complex (**Figures 5C,E, 6A**). PKC ϵ , MnSOD, and VEGF were decreased in the MV endothelium in age-related memory-impaired rats compared to control young rats (**Figures 5D,F, 6B**). Bryostatin abolished the aging-dependent reduction in PKC ϵ to the young control level (**Figure 5D**). For the effect related to oxidative stress, bryostatin treatment also rescued the aging-dependent decreases in MnSOD and even increased MnSOD higher than the level in young rats (**Figure 5F**). For the effect on angiogenesis, the reduction of VEGF in aged rats was reversed with bryostatin



treatment (**Figure 6B**). We studied MV density using the IB4 at low magnification confocal microscopy. Change in MV density was determined with quantification of the IB4 area within hippocampal CA1 stratum radiatum (**Figure 6C**). Blood vessels decreased in age-associated memory-impaired rats (**Figure 6D**). The MV loss was rescued in the hippocampus by bryostatin and DCP-LA compared to aged rats without bryostatin or DCP-LA (**Figure 6D**). The results suggest that the decrease in PKC ϵ , MnSOD, and VEGF expression in MV endothelium is associated with the MV loss during age-related



memory impairment. The PKC ϵ activators bryostatin and DCP-LA increase MnSOD and VEGF levels and MV density in aged rats with memory impairment.

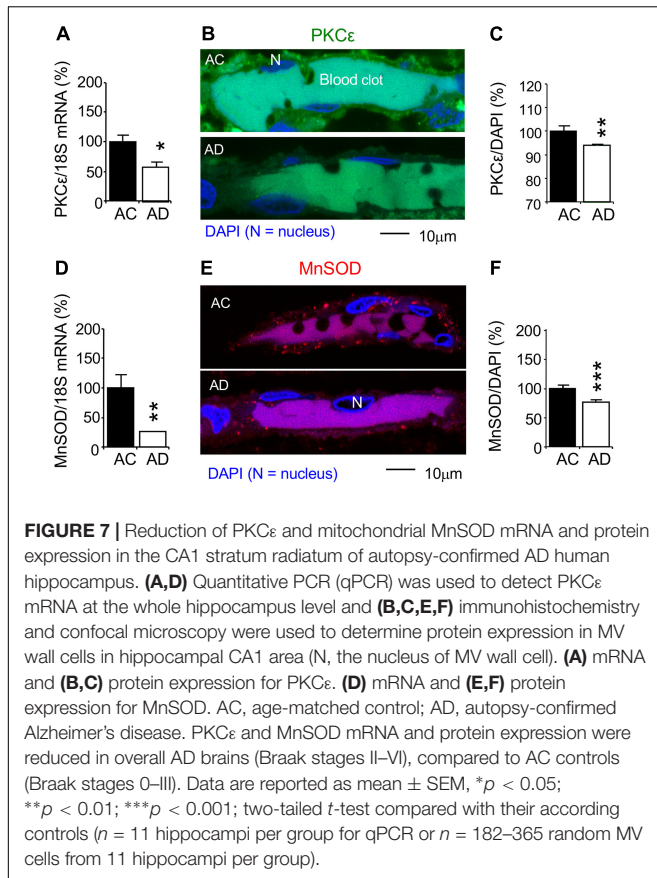
PKC ϵ , Manganese Superoxide Dismutase, and Vascular Endothelial Growth Factor mRNA and Protein Levels and Microvascular Density in Human Autopsy-Confirmed Alzheimer's Disease Hippocampus

Autopsy-confirmed AD brains were collected between 6.83 and 28 h post-mortem (**Table 1**). No significant difference between post-mortem interval and immunohistochemistry (each primary antibody) was seen using linear regression analysis (not shown), suggesting that our results were not affected by post-mortem change within 28 h. The age was 79.4 ± 9.9 (mean \pm S.E) years for AD brains, compared to 78.7 ± 11.4 years for age and gender-matched control (AC) brains. The Braak staging was 4.3 ± 0.4 (range = II–VI) for AD brains, compared to 1.4 ± 0.2 (range = 0–III) for AC brains.

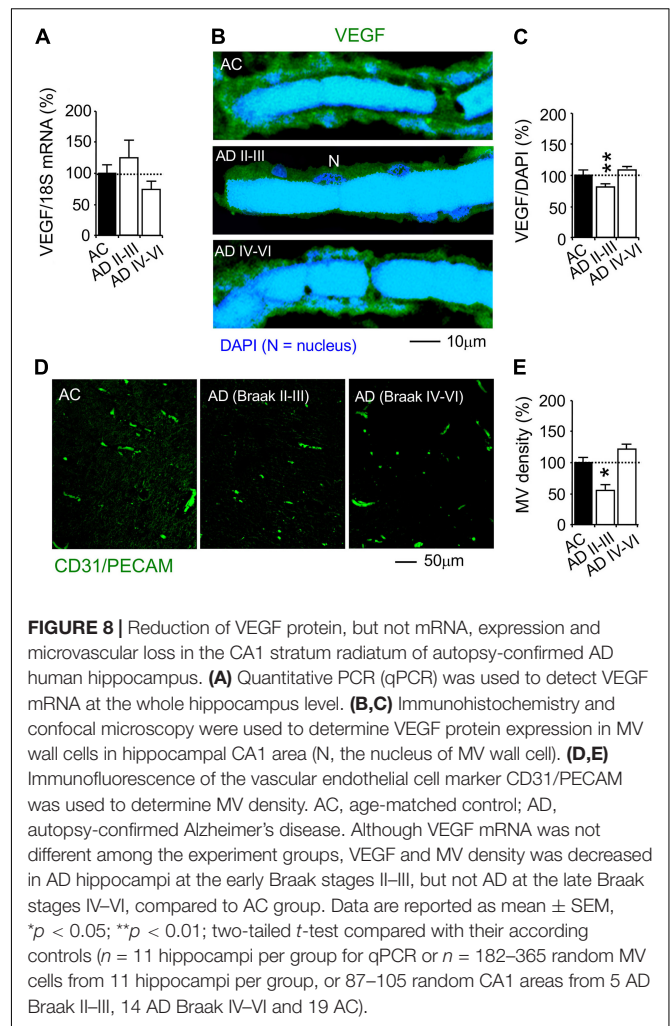
Changes in PKC ϵ , MnSOD, and VEGF were studied in AD subjects (n = 11) and AC controls (n = 11). AC control data were set at 100%, and all other experiment data were defined as % of their AC controls. qPCR was used to determine change in mRNAs at the whole hippocampal level. The PKC ϵ and MnSOD

TABLE 1 | Demographic data of human brains.

Diagnosis	Braak	Age (year)	Gender	PMI (h)
Control	0	61	F	16.80
Control	I	69	M	18.43
Control	I	73	M	20.88
Control	I	75	F	20.08
Control	I	76	M	12.25
Control	I	81	F	26.18
Control	I	82	F	15.70
Control	II	84	F	19.25
Control	II	86	M	25.28
Control	II	97	M	17.00
Control	III	89	F	14.12
AD	II	72	M	6.83
AD	II/III	80	M	23.17
AD	II/III	71	M	28
AD	III/IV	83	F	5.9
AD	IV	88	F	16.67
AD	IV	98	M	22.70
AD	V	61	F	21.42
AD	V	68	M	15.67
AD	V	73	F	17.67
AD	V	81	F	20.75
AD	V	82	F	18
AD	V	80	M	15
AD	VI	87	M	15.25

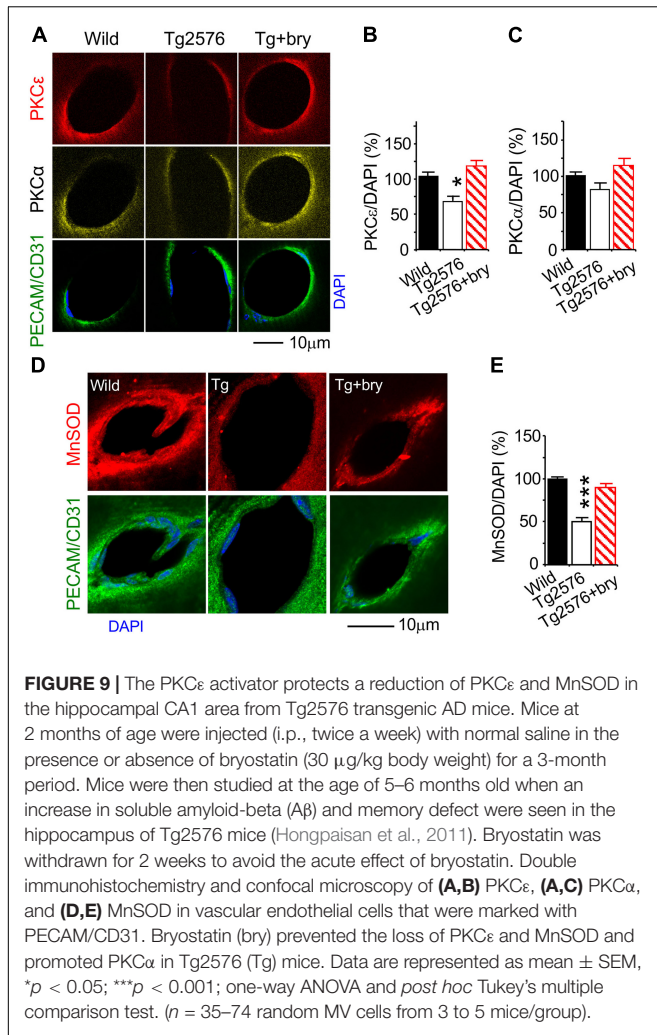


mRNAs were reduced in the AD hippocampus compared to the AC control (**Figures 7A,D**). Immunohistochemistry and confocal microscopy were used to determine protein changes in the



MV endothelium in the hippocampal CA1 stratum radiatum (**Figures 7B,E**). In parallel to changes in mRNA expression at the whole hippocampal level, MV endothelium in the hippocampus showed a decrease in PKC ϵ and mitochondrial MnSOD levels (**Figures 7C,F**). The results indicate that AD pathogenesis is involved in the damage of PKC ϵ and MnSOD mRNA expression, resulting in a decrease in PKC ϵ and MnSOD translation.

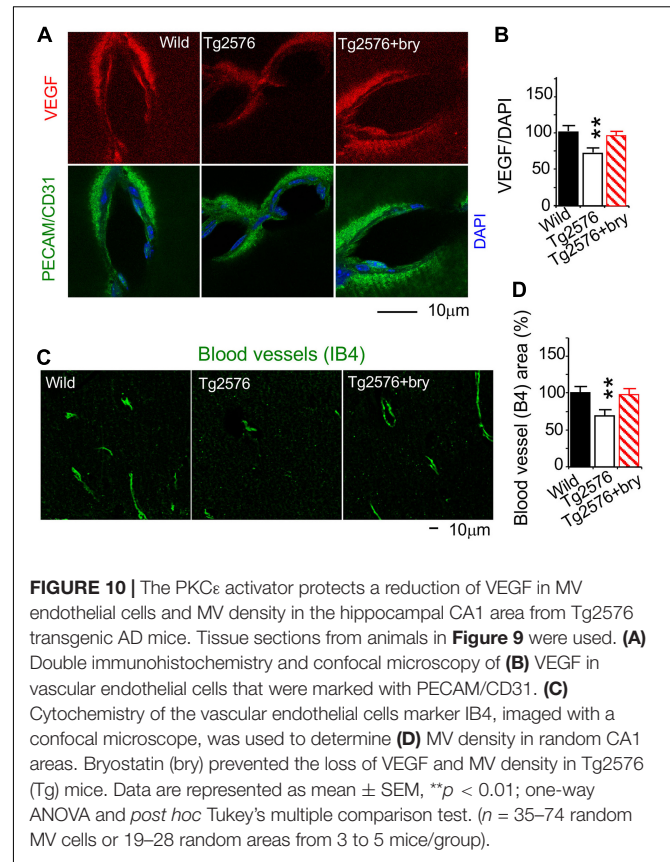
Although VEGF mRNA was not changed in AD hippocampi (**Figure 8A**), VEGF protein expression in the MV wall cells was reduced in the AD hippocampi at Braak stages II–III, but not AD stages IV–VI, compared to the AC controls (Braak stages 0–III, **Figures 8B,C**). This suggests that AD pathogenesis is associated with decreased VEGF synthesis and/or increased VEGF degradation. Using immunohistochemistry of the vascular endothelial marker PECAM-1/CD31, overall MV area density was determined as % of MV fraction in random areas of the hippocampal CA1 radiatum (**Figure 8D**). The MV area in the AD hippocampi was decreased at Braak stages II–III, but not Braak stages IV–VI (**Figure 8E**). The results indicate that a decrease in PKC ϵ , MnSOD and VEGF expression and the loss of microvessels is associated with AD pathogenesis.



Effect of the PKC ϵ Activator on Vascular Manganese Superoxide Dismutase and Vascular Endothelial Growth Factor in the Hippocampi of Alzheimer's Disease Transgenic Mice Tg2576

Function effect of PKC ϵ was studied in animal models treated with the PKC ϵ activator drug, bryostatin. The effect of PKC ϵ on MV density, VEGF, and MnSOD was studied in Tg2576 transgenic AD mice that overexpress a mutant form of APP (isoform 695) with the Swedish mutation (KM670/671NL). Double immunohistochemistry and confocal microscopy were used to evaluate PKC ϵ , PKC α , MnSOD, and VEGF levels in vascular endothelial cells marked with platelet endothelial cell adhesion molecule (PECAM-1) or cluster of differentiation 31 (CD31) (Figures 9A,D, 10A).

Because bryostatin is a potent activator of PKC ϵ and to a lesser extent PKC α (Hongpaisan and Alkon, 2007), changes in PKC ϵ and PKC α were determined. Compared to the wild-type control mice, PKC ϵ level in Tg2576 mice was decreased in MV endothelial cells that were treated with bryostatin (Figures 9A,B).



Although PKC α concentration was not changed in Tg2576 mice, bryostatin significantly increased PKC α (Figures 9A,C). MnSOD was decreased in MV endothelial cells in Tg2576 mice compared to wild-type controls (Figures 9D,E). Treatment with bryostatin prevented the decrease in MnSOD (Figures 9D,E).

We further determined change of VEGF level. Compared to wild-type littermate sibling mice, a reduction of VEGF in MV endothelial cells in Tg2576 mice was prevented after bryostatin treatment (Figures 10A,B). IB4 histochemistry was used to determine MV density (Figure 10C). The PKC ϵ activator bryostatin prevented the MV loss in Tg2576 mice (Figure 10D). Taken together, the results suggest that the PKC ϵ activator can prevent the decrease in PKC ϵ MnSOD and VEGF levels and in MV loss in AD transgenic mice Tg2576.

DISCUSSION

The present study demonstrated that the TBHP-induced short-term oxidative stress decreased MnSOD—but not PKC ϵ and VEGF—mRNA and protein expression in cultured HBMEC cells that were blocked by superoxide degrading drugs, Nac and MnTMPyP. The PKC ϵ can increase PKC ϵ mRNA and its protein expression and increase MnSOD mRNA, MnSOD, and VEGF expression, promoted by the mRNA-stabilizing protein HuR that bind ARE sequence in MnSOD and VEGF mRNAs. Under chronic conditions in animal models, reduced PKC ϵ was

associated with a decrease in MnSOD and VEGF expression in MV endothelial cells and MV density in the hippocampi of aged rats (>24 months old) and young AD transgenic mice Tg2576 (5–6 months old). The PKC ϵ activators DCP-LA and bryostatin rescued the reduction of PKC ϵ , MnSOD, and VEGF in MV cells and the MV loss.

During the aging process, the activity of sirtuin1 (SIRT1) in the nucleus is reduced, which decreases the von Hippel-Lindau (pVHL) protein levels and subsequently stabilizes hypoxia-inducible factor-1 α (HIF-1 α). Activated HIF-1 α reduces the proliferator-activated receptor-gamma coactivator 1 β (PGC-1 β) activity, resulting in the downregulation of mitochondrial genes and MnSOD (Lu et al., 2010; Yeo, 2019). c-Myc activity is also inhibited upon its interaction with HIF-1 α . c-Myc targets gene-regulating processes required for cell growth, including rRNA transcription and processing, ribosomal protein transcription and translation, and translation initiation (Lu et al., 2010). The reduction of c-Myc activity may elicit the loss of VEGF (Baudino et al., 2002; Florea et al., 2013). In the present study, it is likely that the PKC ϵ activator may have increased SIRT1 and c-Myc, resulting in the increase in MnSOD mRNA transcription during oxidative stress (Li et al., 1996; Thompson et al., 2013).

In the present study, normal aging and AD pathogenesis were associated with a decrease in PKC ϵ , MnSOD, and VEGF, possibly due to a prolonged and significant increase in O₂^{•-} that favors reaction with the free radical nitric oxide (NO[•]) to form peroxynitrite (ONONO₂⁻), a powerful oxidant that damages DNA, RNA, and proteins, including PKC (Maher, 2001). On the other hand, the PKC ϵ activator can restore the mitochondria antioxidant MnSOD that may buffer oxidative stress and may inhibit the oxidative damage of PKC ϵ and VEGF. It has been previously shown that the PKC ϵ activators can increase PKC ϵ itself; however, the mechanism is not clearly understood (Hongpaisan et al., 2011, 2013).

In a previous study, we showed that DCP-LA and/or bryostatin improved recent memory retention, which is important for daily living activity, by restoring the reduction of PKC ϵ accumulation in axonal and presynaptic axonal boutons and improving synaptic formation/modification in aged rats and AD transgenic mice Tg2576 and 5xFAD. This was done by preventing/improving PKC ϵ -activated mRNA-stabilizing protein HuD or ELAV-like protein 4, which inhibits mRNA degradation and promotes MnSOD and BDNF in hippocampal neurons (Hongpaisan et al., 2011, 2013; Sen et al., 2018). PKC ϵ is critical in synaptogenesis and memory (Prekeris et al., 1998; Aranda-Abreu et al., 1999; Hama et al., 2004), and the present study demonstrated that DCPLA and bryostatin can rescue the loss of blood vessels by preventing and/or restoring the loss of PKC ϵ , MnSOD, and VEGF that may contribute to improved learning acquisition and memory retention in animal models of normal aging (as shown in the present study) and AD transgenic mice Tg2576 and 5xFAD (Hongpaisan et al., 2011, 2013; for review see Govoni et al. (2010), Talman et al. (2016)).

In the present study, the mRNA-stabilizing protein HuR is involved in the effect of PKC ϵ activator by suppressing MnSOD and VEGF mRNA degradation. PKC ϵ may stimulate protein phosphatase 2A (PP2A) to facilitate the dephosphorylation

of phospho-Akt and subsequently lead to the accumulation of the dephosphorylated and active forkhead box O3s (FOXO3a), which activates MnSOD mRNA transcription, while PKC α may phosphorylate the CREB transcription of MnSOD mRNAs (Chung et al., 2011). Binding of VEGF on vascular endothelial growth factor receptor 2 (VEGFR2) can activate the PKC/extracellular signal-regulated kinase (ERK) 1/2 signal cascade. In the present study, the PKC ϵ activator may therefore promote VEGF signaling by directly activating extracellular signal-regulated kinase (ERK) 1/2 and vascular proliferation (Rask-Madsen and King, 2008).

CONCLUSION

During aging and AD pathogenesis, PKC ϵ , MnSOD, and VEGF expression decreases in MV endothelial cells and MV loss occurs in the hippocampus. The PKC ϵ activators can reduce the decrease of PKC ϵ and MnSOD mRNA and protein expression in MV cells. PKC ϵ activators can also increase VEGF, which is important for angiogenesis and blood vessel maintenance.

DATA AVAILABILITY STATEMENT

The original contributions presented in the study are included in the article, further inquiries can be directed to the corresponding author.

ETHICS STATEMENT

The animal study was reviewed and approved by Institutional Animal Care and Use Committee at Thomas Jefferson University.

AUTHOR CONTRIBUTIONS

JH: conceptualization and writing – original draft. GM, HW, ZZ, and JH: formal analysis. GM, HW, ZZ, DA, and JH: writing – review and editing. All authors contributed to the article and approved the submitted version.

FUNDING

Research reported in this publication was supported by the National Institute on Aging of the National Institutes of Health under Award Number R01AG058884.

ACKNOWLEDGMENTS

Human tissue specimens were obtained from the NIH NeuroBioBank: the Harvard Brain Tissue Resource Center

McLean Hospital, Boston, MA, United States; as well as NIH Brain and Tissue Repository-California, Human Brain and Spinal Fluid Resource Center, VA West Los Angeles Medical Center, Los Angeles, CA, United States, which is supported in part by the NIH

and the US Department of Veterans Affairs. We would like to thank Pamela Walter, MFA; the Director of Office for Professional Writing, Publishing, and Communication at Thomas Jefferson University for language editing of this manuscript.

REFERENCES

- Allegrì, L., Baldan, F., Roy, S., Aubé, J., Russo, D., Filetti, S., et al. (2019). The HuR CMLD-2 inhibitor exhibits antitumor effects *via* MAD2 downregulation in thyroid cancer cells. *Sci. Rep.* 9:7374. doi: 10.1038/s41598-019-43894-0
- Amadio, M., Osera, C., Lupo, G., Motta, C., Drago, F., Govoni, S., et al. (2012). Protein kinase C activation affects, *via* the mRNA-binding Hu-antigen R/ELAV protein, vascular endothelial growth factor expression in a pericytic/endothelial coculture model. *Mol. Vis.* 18, 2153–2164. doi: 10.1080/15476286.2015.1085276
- Antic, D., and Keene, J. D. (1998). Messenger ribonucleoprotein complexes containing human ELAV proteins: interactions with cytoskeleton and translational apparatus. *J. Cell Sci.* 111, 183–197. doi: 10.1242/jcs.111.2.183
- Aranda-Abreu, G. E., Behar, L., Chung, S., Furneaux, H., and Ginzburg, I. (1999). Embryonic lethal abnormal vision-like RNA-binding proteins regulate neurite outgrowth and tau expression in PC12 cells. *J. Neurosci.* 19, 6907–6917. doi: 10.1523/JNEUROSCI.19-16-06907.1999
- Arcondeguy, T., Lacazette, E., Millevoi, S., Prats, H., and Touriol, C. (2013). VEGF-A mRNA processing, stability and translation: a paradigm for intricate regulation of gene expression at the post-transcriptional level. *Nucleic Acids Res.* 41, 7997–8010. doi: 10.1093/nar/gkt539
- Arvanitakis, Z., Leurgans, S. E., Barnes, L. L., Bennett, D. A., and Schneider, J. A. (2011). Microinfarct pathology, dementia, and cognitive systems. *Stroke* 42, 722–727. doi: 10.1161/STROKEAHA.110.595082
- Battaini, F., and Pascale, A. (2005). Protein kinase C signal transduction regulation in physiological and pathological aging. *Ann. N.Y. Acad. Sci.* 1057, 177–192. doi: 10.1196/annals.1356.011
- Baudino, T. A., McKay, C., Pendeveille-Samain, H., Nilsson, J. A., Maclean, K. H., White, E. L., et al. (2002). c-Myc is essential for vasculogenesis and angiogenesis during development and tumor progression. *Genes Dev.* 16, 2530–2543. doi: 10.1101/gad.1024602
- Benton, R. L., Maddie, M. A., Minnillo, D. R., Hagg, T., and Whittemore, S. (2008). Griffonia simplicifolia isolectin B4 identifies a specific subpopulation of angiogenic blood vessels following contusive spinal cord injury in the adult mouse. *J. Comp. Neurol.* 507, 1031–1052. doi: 10.1002/cne.21570
- Brown, W. R., and Thore, C. R. (2011). Review: cerebral microvascular pathology in aging and neurodegeneration. *Neuropathol. Appl. Neurobiol.* 37, 56–74. doi: 10.1111/j.1365-2990.2010.01139.x
- Chattopadhyay, R., Dyukova, E., Singh, N. K., Ohba, M., Mobley, J. A., and Rao, G. N. (2014). Vascular endothelial tight junctions and barrier function are disrupted by 15(S)-hydroxyicosatetraenoic acid partly *via* protein kinase C epsilon-mediated zona occludens-1 phosphorylation at threonine 770/772. *J. Biol. Chem.* 289, 3148–3163. doi: 10.1074/jbc.M113.528190
- Chaudhuri, L., Nicholson, A. M., Kalen, A. L., and Goswami, P. C. (2012). Preferential selection of MnSOD transcripts in proliferating normal and cancer cells. *Oncogene* 31, 1207–1216. doi: 10.1038/ncr.2011.325
- Chung, S., Eckrich, M., Perrone-Bizzozero, N., Kohn, D. T., and Furneaux, H. (1997). The ELAV-like proteins bind to a conserved regulatory element in the 3'-untranslated region of GAP-43 mRNA. *J. Biol. Chem.* 272, 6593–6598. doi: 10.1074/jbc.272.10.6593
- Chung, Y. W., Kim, H. K., Kim, I. Y., Yim, M. B., and Chock, P. B. (2011). Dual function of protein kinase C (PKC) in 12-O-tetradecanoylphorbol-13-acetate (TPA)-induced manganese superoxide dismutase (MnSOD) expression: activation of CREB and FOXO3a by PKC-alpha phosphorylation and by PKC-mediated inactivation of Akt, respectively. *J. Biol. Chem.* 286, 29681–29690. doi: 10.1074/jbc.M111.264945
- Davis, G. E., Koh, W., and Stratman, A. N. (2007). Mechanisms controlling human endothelial lumen formation and tube assembly in three-dimensional extracellular matrices. *Birth Defects Res. C Embryo Today* 81, 270–285. doi: 10.1002/bdrc.20107
- Desai, B. S., Schneider, J. A., Li, J.-L., Carvey, P. M., and Hendey, B. (2009). Evidence of angiogenic vessels in Alzheimer's disease. *J. Neurol. Transm.* 116, 587–597. doi: 10.1007/s00702-009-0226-9
- Di Marcantonio, D., Martinez, E., Sidoli, S., Vadaketh, J., Nieborowska-Skorska, M., Gupta, A., et al. (2018). Protein kinase C epsilon is a key regulator of mitochondrial redox homeostasis in acute myeloid leukemia. *Clin. Cancer Res.* 24, 608–618. doi: 10.1158/1078-0432.CCR-17-2684
- El Assar, M., Angulo, J., and Rodriguez-Manas, L. (2013). Oxidative stress and vascular inflammation in aging. *Free Radic. Biol. Med.* 65, 380–401. doi: 10.1016/j.freeradbiomed.2013.07.003
- Elmlinger, M. W., Kriebel, M., and Ziegler, D. (2011). Neuroprotective and anti-oxidative effects of the hemodialysate actovegin on primary rat neurons *in vitro*. *Neuromol. Med.* 13, 266–274. doi: 10.1007/s12017-011-8157-7
- Fedotcheva, N. I., and Mokhova, E. N. (2013). Mechanism of induction of oxidative stress in liver mitochondria by low concentrations of tert-butyl hydroperoxide. *Biochemistry* 78, 75–79. doi: 10.1134/S0006297913010094
- Florea, V., Bhagavatula, N., Simovic, G., Macedo, F. Y., Fock, R. A., and Rodrigues, C. O. (2013). c-Myc is essential to prevent endothelial pro-inflammatory senescent phenotype. *PLoS One* 8:e73146. doi: 10.1371/journal.pone.0073146
- Govoni, S., Amadio, M., Battaini, F., and Pascale, A. (2010). Senescence of the brain: focus on cognitive kinases. *Curr. Pharm. Des.* 16, 660–671. doi: 10.2174/138161210790883732
- Hama, H., Hara, C., Yamaguchi, K., and Miyawaki, A. (2004). PKC signaling mediates global enhancement of excitatory synaptogenesis in neurons triggered by local contact with astrocytes. *Neuron* 41, 405–415. doi: 10.1016/s0896-6273(04)00007-8
- Harman, D. (1956). Aging: a theory based on free radical and radiation chemistry. *J. Gerontol.* 11, 298–300. doi: 10.1093/geronj/11.3.298
- Hawkes, C. A., Härtig, W., Kacza, J., Schliebs, R., Weller, R. O., Nicoll, J. A., et al. (2011). Perivascular drainage of solutes is impaired in the ageing mouse brain and in the presence of cerebral amyloid angiopathy. *Acta Neuropathol.* 121, 431–443. doi: 10.1007/s00401-011-0801-7
- Hongpaisan, J., and Alkon, D. L. (2007). A structural basis for enhancement of long-term associative memory in single dendritic spines regulated by PKC. *Proc. Natl. Acad. Sci. U.S.A.* 104, 19571–19576. doi: 10.1073/pnas.0709311104
- Hongpaisan, J., Sun, M. K., and Alkon, D. L. (2011). PKC epsilon activation prevents synaptic loss, Abeta elevation, and cognitive deficits in Alzheimer's disease transgenic mice. *J. Neurosci.* 31, 630–643. doi: 10.1523/JNEUROSCI.5209-10.2011
- Hongpaisan, J., Xu, C., Sen, A., Nelson, T. J., and Alkon, D. L. (2013). PKC activation during training restores mushroom spine synapses and memory in the aged rat. *Neurobiol. Dis.* 55, 44–62. doi: 10.1016/j.nbd.2013.03.012
- Kaan, E. B., Dara, L. D., Rayshad, G., Franz, F., and Wilfred, A. J. (2013). Cessation of neoangiogenesis in Alzheimer's disease follows amyloid-beta immunization. *Sci. Rep.* 3:1354. doi: 10.1038/srep01354
- Kemper, T., Moss, M. B., Hollander, W., and Prusty, S. (1999). Microinfarction as a result of hypertension in a primate model of cerebrovascular disease. *Acta Neuropathol.* 98, 295–303. doi: 10.1007/s004010051083
- King, P. H. (2000). RNA-binding analyses of HuC and HuD with the VEGF and c-myc 3'-untranslated regions using a novel ELISA-based assay. *Nucleic Acids Res.* 28:e20. doi: 10.1093/nar/28.7.e20
- Laitinen, L. (1987). Griffonia simplicifolia lectins bind specifically to endothelial cells and some epithelial cells in mouse tissues. *Histochem. J.* 19, 225–234. doi: 10.1007/BF01680633
- Lal, P., Cerofolini, L., D'Agostino, V. G., Zucal, C., Fuccio, C., Bonomo, I., et al. (2017). Regulation of HuR structure and function by dihydrotanshinone-I. *Nucleic Acids Res.* 45, 9514–9527. doi: 10.1093/nar/gkx623
- Li, Y., Davis, K. L., and Sytkowski, A. J. (1996). Protein kinase C-epsilon is necessary for erythropoietin's up-regulation of c-myc and for factor-dependent DNA synthesis. Evidence for discrete signals for growth and differentiation. *J. Biol. Chem.* 271, 27025–27030. doi: 10.1074/jbc.271.43.27025

- Lu, Z., Xu, X., Hu, X., Fassett, J., Zhu, G., Tao, Y., et al. (2010). PGC-1 α Regulates expression of myocardial mitochondrial antioxidants and myocardial oxidative stress after chronic systolic overload. *Antioxid. Redox Signal.* 13, 1011–1022. doi: 10.1089/ars.2009.2940
- Maher, P. (2001). How protein kinase C activation protects nerve cells from oxidative stress-induced cell death. *J. Neurosci.* 21, 2929–2938. doi: 10.1523/JNEUROSCI.21-09-02929.2001
- Nunomura, A., Perry, G., Aliev, G., Hirai, K., Takeda, A., Balraj, E. K., et al. (2001). Oxidative damage is the earliest event in Alzheimer disease. *J. Neuropathol. Exp. Neurol.* 60, 759–767. doi: 10.1093/jnen/60.8.759
- Pascale, A., Amadio, M., Scapagnini, G., Lanni, C., Racchi, M., Provenzani, A., et al. (2005). Neuronal ELAV proteins enhance mRNA stability by a PKC α -dependent pathway. *Proc. Natl. Acad. Sci. U.S.A.* 102, 12065–12070. doi: 10.1073/pnas.0504702102
- Pascale, A., Gusev, P. A., Amadio, M., Dottorini, T., Govoni, S., Alkon, D. L., et al. (2004). Increase of the RNA-binding protein HuD and posttranscriptional up-regulation of the GAP-43 gene during spatial memory. *Proc. Natl. Acad. Sci. U.S.A.* 101, 1217–1222. doi: 10.1073/pnas.0307674100
- Prekeris, R., Hernandez, R. M., Mayhew, M. W., White, M. K., and Terrian, D. M. (1998). Molecular analysis of the interactions between protein kinase C γ and filamentous actin. *J. Biol. Chem.* 273, 26790–26798. doi: 10.1074/jbc.273.41.26790
- Qosa, H., LeVine, I. I. H., Keller, J. N., and Kaddoumi, A. (2014). Mixed oligomers and monomeric amyloid-beta disrupts endothelial cells integrity and reduces monomeric amyloid-beta transport across hCMEC/D3 cell line as an *in vitro* blood-brain barrier model. *Biochim. Biophys. Acta* 1842, 1806–1815. doi: 10.1016/j.bbdis.2014.06.029
- Quattrone, A., Pascale, A., Noguez, X., Zhao, W., Gusev, P., Pacini, A., et al. (2001). Posttranscriptional regulation of gene expression in learning by the neuronal ELAV-like mRNA-stabilizing proteins. *Proc. Natl. Acad. Sci. U.S.A.* 98, 11668–11673. doi: 10.1073/pnas.191388398
- Rask-Madsen, C., and King, G. L. (2008). Differential regulation of VEGF signaling by PKC α and PKC ϵ in endothelial cells. *Arterioscler. Thromb. Vasc. Biol.* 28, 919–924. doi: 10.1161/ATVBAHA.108.162842
- Riddle, D. R., Sonntag, W. E., and Lichtenwalner, R. J. (2003). Microvascular plasticity in aging. *Ageing Res. Rev.* 2, 149–168. doi: 10.1016/s1568-1637(02)00064-8
- Sanz, A., and Stefanatos, R. K. (2008). The mitochondrial free radical theory of aging: a critical view. *Curr. Aging Sci.* 1, 10–21. doi: 10.2174/1874609810801010010
- Sen, A., Alkon, D. L., and Nelson, T. J. (2012). Apolipoprotein E3 (ApoE3) but not ApoE4 protects against synaptic loss through increased expression of protein kinase C epsilon. *J. Biol. Chem.* 287, 15947–15958. doi: 10.1074/jbc.M111.312710
- Sen, A., and Hongpaisan, J. (2018). Hippocampal microvasculature changes in association with oxidative stress in Alzheimer's disease. *Free Radic. Biol. Med.* 120, 192–203. doi: 10.1016/j.freeradbiomed.2018.03.034
- Sen, A., Nelson, T. J., Alkon, D. L., and Hongpaisan, J. (2018). Loss in PKC epsilon causes downregulation of MnSOD and BDNF expression in neurons of Alzheimer's disease hippocampus. *J. Alzheimers Dis.* 63, 1173–1189. doi: 10.3233/JAD-171008
- Sonobe, Y., Takeuchi, H., Kataoka, K., Li, H., Jin, S., Mimuro, M., et al. (2009). Interleukin-25 expressed by brain capillary endothelial cells maintains blood-brain barrier function in a protein kinase C epsilon-dependent manner. *J. Biol. Chem.* 284, 31834–31842. doi: 10.1074/jbc.M109.025940
- Talman, V., Pascale, A., Jäntti, M., Amadio, M., and Tuominen, R. K. (2016). Protein kinase C activation as a potential therapeutic strategy in Alzheimer's disease: is there a role for embryonic lethal abnormal vision-like proteins? *Basic Clin. Pharmacol. Toxicol.* 119, 149–160. doi: 10.1111/bcpt.12581
- Thompson, J. W., Dave, K. R., Saul, I., Narayanan, S. V., and Perez-Pinzon, M. A. (2013). Epsilon PKC increases brain mitochondrial SIRT1 protein levels via heat shock protein 90 following ischemic preconditioning in rats. *PLoS One* 8:e75753. doi: 10.1371/journal.pone.0075753
- Toda, N. (2012). Age-related changes in endothelial function and blood flow regulation. *Pharmacol. Ther.* 133, 159–176. doi: 10.1016/j.pharmthera.2011.10.004
- Ungvari, Z., Tarantini, S., Kiss, T., Wren, J. D., Giles, C. B., Griffin, C. T., et al. (2018). Endothelial dysfunction and angiogenesis impairment in the ageing vasculature. *Nat. Rev. Cardiol.* 5, 555–565. doi: 10.1038/s41569-018-0030-z
- Wang, W., Yang, X., Cristofalo, V. J., Holbrook, N. J., and Gorospe, M. (2001). Loss of HuR is linked to reduced expression of proliferative genes during replicative senescence. *Mol. Cell. Biol.* 21, 5889–5898. doi: 10.1128/MCB.21.17.5889-5898.2001
- Yeo, E.-J. (2019). Hypoxia and aging. *Exp. Mol. Med.* 51, 1–15. doi: 10.1038/s12276-019-0233-3
- Zielonka, J., and Kalyanaraman, B. (2010). Hydroethidine- and mitoSOX-derived red fluorescence is not a reliable indicator of intracellular superoxide formation: another inconvenient truth. *Free Radic. Biol. Med.* 48, 983–1001. doi: 10.1016/j.freeradbiomed.2010.01.028

Conflict of Interest: DA was employed by Neurotrope Bioscience, Inc.

The remaining authors declare that the research was conducted in the absence of any commercial or financial relationships that could be construed as a potential conflict of interest.

Publisher's Note: All claims expressed in this article are solely those of the authors and do not necessarily represent those of their affiliated organizations, or those of the publisher, the editors and the reviewers. Any product that may be evaluated in this article, or claim that may be made by its manufacturer, is not guaranteed or endorsed by the publisher.

Copyright © 2022 Millien, Wang, Zhang, Alkon and Hongpaisan. This is an open-access article distributed under the terms of the Creative Commons Attribution License (CC BY). The use, distribution or reproduction in other forums is permitted, provided the original author(s) and the copyright owner(s) are credited and that the original publication in this journal is cited, in accordance with accepted academic practice. No use, distribution or reproduction is permitted which does not comply with these terms.